



Published in final edited form as:

Mol Cancer Res. 2016 March ; 14(3): 253–266. doi:10.1158/1541-7786.MCR-15-0361.

A DNA-binding Molecule Targeting the Adaptive Hypoxic Response in Multiple Myeloma has Potent Anti-tumor Activity

Veena S. Mysore^{1,2}, Jerzy Szablowski³, Peter B. Dervan³, and Patrick J. Frost^{1,2,*}

¹Greater Los Angeles Veteran Administration Healthcare System, Los Angeles, CA 90073

²University of California, Los Angeles, Los Angeles, CA 90024

³Division of Chemistry & Chemical Engineering, California Institute of Technology, Pasadena, CA 91125

Abstract

Multiple myeloma (MM) is incurable and invariably becomes resistant to chemotherapy. Although the mechanisms remain unclear, hypoxic conditions in the bone marrow have been implicated in contributing to MM progression, angiogenesis, and resistance to chemotherapy. These effects occur via adaptive cellular responses mediated by hypoxia-inducible transcription factors (HIFs), and targeting HIFs can have anti-cancer effects in both solid and hematological malignancies. Here, it was found that in most myeloma cell lines tested, HIF1 α , but not HIF2 α expression was oxygen dependent and this could be explained by the differential expression of the regulatory prolyl-hydroxylase isoforms. The anti-MM effects of a sequence-specific DNA-binding pyrrole-imidazole polyamide (HIF-PA), that disrupts the HIF heterodimer from binding to its cognate DNA sequences, were also investigated. HIF-PA is cell permeable, localizes to the nuclei, and binds specific regions of DNA with an affinity comparable to that of HIF transcription factors. Most of the MM cells were resistant to hypoxia-mediated apoptosis, and HIF-PA treatment could overcome this resistance *in vitro*. Using xenograft models, it was determined that HIF-PA significantly decreased tumor volume and increased hypoxic and apoptotic regions within solid tumor nodules and the growth of myeloma cells engrafted in the bone marrow. This provides a rationale for targeting the adaptive cellular hypoxic response of the O₂-dependent activation of HIF α using polyamides.

Keywords

mTOR; multiple myeloma; hypoxia

*Corresponding author: Patrick Frost, Ph.D, Department of Hematology-Oncology, Greater Los Angeles VA Healthcare System, 11301 Wilshire Blvd, Los Angeles, CA, 90073., Phone=310-478-3711 ext 40410, Fax=310-268-3190, Patrick.Frost@va.gov.

CONFLICT OF INTEREST: The authors have no conflict of interest to report.

DISCLAIMER: These contents do not necessarily represent the views of the US Department of Veterans Affairs or the US Government

INTRODUCTION

Multiple myeloma (MM) is an incurable disease of malignant plasma cells characterized by high rates of relapse and resistance to drug therapies (1–3). The reasons why this disease is so difficult to cure is unclear, but the bone marrow (BM) microenvironment is known to confer critical growth and survival advantages that protect tumor cells from apoptosis-inducing stressors (4, 5). The BM is hypoxic ($pO_2 \sim 10\text{--}30$ mmHg) when compared to most other tissues ($pO_2 \sim 85\text{--}150$ mmHg) (6) and paradoxically, while oxygen stress can kill tumor cells (7), low-oxygen conditions also promote tumor progression (8), angiogenesis (9), and resistance to chemotherapy (10). These pro-survival responses to low oxygen tension are regulated by adaptive cellular responses mediated by several oxygen-sensitive transcription factors; the most important of these being the hypoxia-inducible factors (HIFs) (for review see (11)). HIFs are composed of a constitutively expressed β -subunit (HIF1 β /ARNT) and inducible α -subunits (HIF1 α , 2 α , and 3 α) that are responsive to oxygen levels and are regulated via proteasome-mediated degradation. Briefly, under “normoxic” conditions, the HIF α subunits are hydroxylated by a number of closely related prolyl-hydroxylase domain proteins (PHD1-3) that results in recognition of the α -subunit by the von Hippel-Lindau tumor suppressor (VHL), and its subsequent ubiquitination and rapid degradation by the proteasome. This normally maintains the HIF α -subunits at very low levels in the cell. Under hypoxic conditions ($pO_2 < 50$ mmHg), the proline-hydroxylase activity is inhibited and HIF α degradation is not initiated (12). This allows dimerization of the α and β -subunits and the translocation and binding of HIF to the hypoxic response elements (HRE), thereby inducing gene transcription of hypoxia related survival and angiogenic factors.

It has been shown that heightened expression of pro-angiogenic factors (such as VEGF) and increased microvessel density within myeloma tumors is strongly correlated with disease development and progression, as well as being predictive of poor patient prognosis (13–16). This provided a rationale for using VEGF-targeting drugs, such as bevacizumab (Avastin), to attempt to inhibit angiogenesis and increase hypoxic stress in MM tumors, although only modest anti-tumor effects were observed (17). These results call into question the overall effectiveness of targeting angiogenesis as a mono-therapeutic strategy for treating MM in the clinic. Noting that the increase of hypoxia within the tumor bed following inhibition of VEGF results in the subsequent activation of the adaptive hypoxic response and induction of survival factors may provide an explanation for these underwhelming effects. Under this hypothesis, we would argue that these resultant hypoxic conditions are actually supportive of MM progression (because low O_2 represents a natural component of the bone marrow niche in which myeloma engraft) by maintaining hyperactive HIF activity. Thus, rather than killing the tumor cells, inhibition of angiogenesis may actually facilitate a pro-survival adaptive hypoxic response through HIF activation. If true, then targeting the specific HIF-mediated response to hypoxia may be a more effective anti-myeloma therapy than targeting VEGF or angiogenesis alone. In fact, there are a number of different hypoxia and HIF targeting strategies currently being tested in MM with varying levels of success (18).

In this study, we tested the effects of inhibiting the hypoxic adaptive response using a synthetically derived, sequence-specific DNA-binding Py-Im polyamide (PA) composed of

the aromatic rings of N-methylpyrrole and N-methylimidazole amino acids designed to recognize and interfere with HIF binding to HRE sequences within the minor groove of the DNA helix (19). We found that under low oxygen culturing conditions, most myeloma cell lines were relatively resistant to hypoxia-mediated apoptosis and that HIF1 α , but not HIF2 α , was upregulated in an oxygen-dependent manner. Treatment of MM cells with our HIF-polyamide (HIF-PA) overcame resistance to hypoxia-mediated apoptosis *in vitro* as well as inhibited the transcription of multiple hypoxia-induced genes. We also found that combination treatment with HIF-PA polyamides (to inhibit gene transcription) and the mTOR inhibitor rapamycin (to inhibit gene translation) was markedly more effective at overcoming resistance to hypoxia-mediated apoptosis in MM cells. In additional experiments, we used xenograft models to study the anti-MM effects of Py-Im polyamide treatment on MM tumors *in vivo* and found that Py-Im polyamides were well tolerated by the mice and had a marked anti-tumor effect characterized by a significant increase in hypoxia as well as concomitant increases in apoptotic and necrotic regions within solid tumor nodules as well as inhibition of myeloma growth in tumors engrafted in the BM. Altogether, these data suggest that sensitivity of myeloma to polyamide therapy may be related to the inhibition of gene expression induced by the oxygen-dependent activation of HIF1 α (but not necessarily HIF2 α) and provides a rationale for targeting the adaptive hypoxic responses in MM using these compounds.

MATERIALS AND METHODS

Cell lines and reagents

All cell lines were purchased from ATCC and maintained at 37°C and 5% CO₂ (“normoxic” condition) unless noted. The cell lines were validated using the Johns Hopkins Genetic Core Research Facility (Baltimore, MD) and stock aliquots were stored under liquid nitrogen. Testing for mycoplasma was performed using a mycoplasma PCR detection kit (Sigma-Aldrich, St Louis, MO). Py-Im polyamides were synthesized by solid-phase methods on Kaiser oxime resin (Nova Biochem, Billerica, MA) (20). The tested polyamide, HIF-PA, targets the sequence 5'-WTWCGW-3' (W=A or T) and modulates a subset of hypoxia-induced genes, whilst the control polyamide (CO-PA) recognizes the non-HRE sequence 5'-WGGWCW-3'. Enzyme-linked immunosorbent assay (ELISA) kits specific for human VEGF was purchased from R&D Systems (Minneapolis, MN). The Hypoxyprobe-1 kit was purchased from HPI Inc (Burlington, MA). Cellular apoptosis was measured by flow cytometry using a cleaved caspase-3 kit (BD Biosciences, San Jose, CA). Small inhibitory RNA (siRNA) for HIF1 α (Silencer Select siRNA ID# s6539, gene ID# 3091) and scrambled control RNA (Silencer Select negative control #1 siRNA) were purchased from Ambion (Grand Island, NY). Cells were transfected with siRNA using Lipofectamine-2000 (Life Technologies, Grand Island, NY).

Immunoblots

Protein was isolated and western blot analysis was performed as described previously (21). Nuclear and cytoplasm fractions were isolated using the Thermo Scientific NE-PER™ Nuclear and Cytoplasmic Extraction Kit (Rockford, IL) following the manufacturers instruction. HIF1 α antibody (clone 54/HIF1) was purchased from BD Biosciences. β -tubulin

(clone H-235), LaminA/C (clone 14/LaminAC), BCL-XL (clone H-5), Survivin (clone D-8), BNIP3 (clone ANa40), BCL-2 (clone C-2), goat anti-mouse and goat anti-rabbit IgG horseradish peroxidase-conjugated antibodies were purchased from Santa Cruz Biotechnology (Dallas, TX). BID (rabbit polyclonal), BAX (rabbit polyclonal), AKT-total (clone C67E7), AKT-S473 (clone D9E) and AKT-T308 (clone C31E5E) and the P70-total, P70-T421/S424, and P70-T389 antibody kits were purchased from Cell Signaling Technology (Danvers, MA). MCL-1 (clone 542808) was purchased from R&D systems. REDD1 (clone 1G11) was purchased from Bethyl Laboratories (Montgomery, TX). The EGLN1/PHD2 (rabbit polyclonal), EGLN3/PHD3 (mouse polyclonal), EGLN3/PHD3 positive control (an EGLN3/PHD3 over expressing lysate from HEK293T cells), HIF2 α (rabbit polyclonal), and Factor inhibiting HIF1 (FIH) antibodies (clone 162C) were purchased from NOVUS Biologicals (Littleton, CO).

Hypoxia-treatments

For induction of hypoxia, MM cells were cultured in a humidified Hypoxymy oxygen hypoxia chamber (Grandpair, Heidelberg, Germany). Variable pO₂ levels were established in the hypoxia chamber from 2-0.1% O₂, and 5% CO₂ at 37 °C. Oxygen levels were regularly tested and calibrated using the manufacturer's protocol.

Generation of hypoxia response element luciferase-expressing (HRE-LUC) cell lines

HRE-LUC reporter MM cell lines (8226, U266, OPM-2) were generated by stably transducing cells using the Cignal lentiviral kit (Qiagen, Valencia, CA) followed by selection with hygromycin (350 mg/ml). For the orthotopic xenograft studies, other luciferase-expressing 8226 cells (8226-LUC) were stably transfected with the pGL4.5 luciferase reporter vector (Promega, San Louis Obispo, CA) using an AMAXA Nucleofector Kit (Lonza, Koln Germany) followed by selection with hygromycin (350 mg/ml). The *in vitro* luciferase activity was confirmed and measured using the dual-luciferase reporter assay kit (Promega, San Louis Obispo) in a luminometer. The *in vivo* luciferase activity was measured using the VivoGlo luciferine substrate (Promega).

Real time PCR

Quantitative expression of VEGF was carried out by quantitative real time PCR. RNA was isolated using Triazol (Life Technologies, Carlsbad, CA) and cDNA was synthesized using cDNA synthesis kit (Life Technologies). VEGF mRNA was amplified using VEGF primers (Life Technologies) in an ABI 7300 real time PCR machine (Life Technologies). The Applied Biosystems® TaqMan® Array Human Hypoxia 96-well Plate was used to test for changes in hypoxia signaling associated genes.

Animals

Male NOD/SCID or NOG mice (4–6 weeks old) were obtained from Jackson Laboratories (Bar Harbor, ME, USA). All animal studies were conducted in accordance with protocols approved by the Institutional Animal Care and Use Committee (IACUC) of the Greater Los Angeles Veterans Administration Healthcare System (GLA-VAHS).

SQ Xenograft Model

We used the murine myeloma xenograft model of Leblanc et al (22) with minor modifications (21). The 8226 cells (10×10^6 cells/mouse) were mixed with matrigel (BD biosciences) then injected subcutaneously into the right flank (200 μ l/mouse) of the mice. The mice were monitored and randomized into drug treated or control groups (10 mice/group) when the tumor volume reached approximately 300–500 mm³. The Py-Im polyamide solution was prepared as previously described (23). Mice were given HIF-PA injections IP every other day for a total of 5 injections. The tumor volume was measured using calipers (width and length) using the formula $W^2 \times (L/2)$ (21, 24) every other day during the course of the experiment.

Orthotopic Xenograft Model

8226-LUC cells were injected (10×10^6 cells/mouse) through the tail vein (200 μ l/injection). In our initial experiments, the localization of human 8226 myeloma cell lines in the bone marrow was determined by two methods: (1) flow cytometry staining of bone marrow aspirates from the femurs of mice using FITC labeled anti-human CD45 antibodies (BD Biosciences) and (2) immunohistochemistry of femurs using anti-human CD45 antibodies. Real time 8226-LUC engraftment in the bone marrow was measured in anesthetized mice given an IP injection of VivoGlo luciferin substrate (100 mg/kg mouse) and then monitored for luciferase activity in the skeleton using a Perkin-Elmer IVIS XRMS small animal imaging system. Luciferase activity in the skeleton of mice challenged with 8226-LUC was typically observed between day +15 and day +20 post challenge. Once a positive bioluminescent signal was observed, the animals were randomized into groups (6–8 animals/group) and were treated with HIF-PA or vehicle control as described above, except a total of 6 injections were given, rather than 5. The luciferase activity was measured twice/week as described above and the change in average radiance (photons/sec/cm²/steradian) was measured and analyzed using the LivingImage version 4.4 imaging software.

Immunohistochemistry

For studies in our SQ model, 24 hours after the last injections, the mice were euthanized and the tumor mass was excised. The tumor was bisected using a razor blade: one half of the tumor was immediately placed in 10% buffered formaldehyde overnight, and the other half was flash frozen for protein extraction. Formaldehyde fixed tumors were embedded in paraffin and cut into 5 μ m-thick serial sections using standard histological procedures. Immunohistochemical staining with cleaved caspase 3, and Hypoxyprobe (pimonidazole) (HPI Inc) was conducted using standardized automated methods.

Morphometric Analysis

IHC analysis was performed on tissue sections with a Nikon Microphot-SA microscope (Melville, NY, USA) equipped with plan-apochromat lenses (20X and 40X). A Diagnostic Technologies digital camera, model SPOT-RT was used to capture images with a resolution of 1520×1080 pixels. Fields were selected by reviewing the slides at low power by a researcher (VM) blinded to the treatments. Multiple non-overlapping fields were identified for analysis of regions of hypoxia/necrosis and apoptotic index at higher powers within these

areas of interest. ImageJ software (NIH, USA) was used to measure percent of hypoxia stained tumor sections. Final images for publication were prepared using Adobe Photoshop software.

Oncomine Analysis

The expression level of *PHD2/EGLN1* and *PHD3/EGLN3* genes in normal, MGUS and MM tumors were analyzed using Oncomine, a cancer microarray database and web-based data-mining platform (25). In order to reduce our false discovery rate, we selected $p < 0.0001$ as a threshold. We analyzed the results for p-values and fold change of our genes of interest.

Statistics

Data was screened for consistency and quality by both graphical (histograms, scatter plots) and analytical methods (descriptive statistics). Variables were analyzed using generalized linear models (GLM) such as ANOVA and *t*-tests. The effect of combining HIF-PA with rapamycin on induction of apoptosis was assessed by the median effect method using Calcsyn Software Version 1.1 (Biosoft, Cambridge, United Kingdom). Combination indices (CI) values were calculated using the most conservative assumption of mutually nonexclusive drug interactions. CI values were calculated from median results of apoptosis assays.

RESULTS

Myeloma cell lines are resistant to hypoxia-induced apoptosis *in vitro*

Because patient MM tumor cells specifically engraft within the hypoxic BM microenvironment, we anticipated that patient-derived MM cell lines would also exhibit resistance to hypoxia-mediated apoptosis *in vitro*. This was confirmed by analyzing the sensitivity of a panel of MM cell lines cultured under various pO_2 concentrations in increments from 2% down to 0.1% O_2 and for various time points up to 72 hours. We chose these experimental ranges because these values fell within the actual pO_2 ranges reported by Spencer et al (6) from *in situ* measurement in mouse bone marrow. In their study, O_2 levels in the marrow were found to be < 32 mm Hg, but in some bone marrow niches, it could be as low as 9.9 mm Hg (or about 1% O_2 with a range of 2 - 0.6% measured in the extra-vascular spaces). We found that at O_2 levels greater than ~1%, only modest cytotoxicity was observed, even when cells were cultured out to 72 hours. Only at very low oxygen conditions (i.e. 0.5 – 0.1% O_2), did we see significant levels of hypoxia-mediated apoptosis of the MM cells tested when compared to the “normoxia-cultured” controls. As shown in Fig 1A, 8226 and U266 cell lines were the most resistant to low pO_2 (~15–20% apoptosis), whilst H929 and MM1.S were intermediately sensitive (~25–35% apoptosis) to hypoxia-mediated apoptosis (all measured at 72 hours). In contrast, OPM-2 cells were the most sensitive (>50% apoptosis) to low O_2 , and this effect occurred significantly earlier, by 48 hours.

Culturing cells under low pO_2 had different effects on the HIF α -subunits expression in the nuclear and cytoplasmic fractions of the hypoxia-resistant (8226) and hypoxia-sensitive (OPM-2) cell lines cultured under standard normoxic (~22% O_2) or hypoxic (0.1% O_2)

conditions. As shown in Fig 1B (left panel), HIF1 α was constitutively expressed in the nuclear fraction of 8226 cells as well as significantly upregulated under hypoxic conditions (measured at 24 hours). In contrast to 8226, baseline HIF1 α was absent in OPM-2 cells, but was strongly induced by low O₂ (Fig 1B, right panel). On the other hand, HIF2 α was constitutively expressed in both 8226 and OPM-2 cells and this was independent of O₂-levels (Fig 1B). The rapid upregulation of HIF1 α in OPM-2 cells was confirmed using the hypoxia mimic, CoCl₂, which induced HIF1 α expression by 1 hour and reached a maximum by 18 hours (Fig 1C). A strong O₂-dependent induction of HIF1 α was also noted in MM1S, H929, and U266 cell lines (Fig 1D), while HIF2 α expression was independent of O₂ levels in H929 and U266 cells, but not in MM1S cells. These findings are generally similar to other reports describing HIF expression in MM cells (3, 26). Low pO₂ (0.1% 24hrs) did not affect the expression of the pro-survival factor Bcl-2, but did inhibit Bcl-xl and MCL-1 in OPM-2 and 8226, whilst survivin was only downregulated in OPM-2 cells (Fig 1E). Survivin has been reported to play a role in HIF-regulated survival of MM and may be an important target for future studies (27). Low pO₂ also upregulated the pro-apoptotic factors, BNIP3 (a known HIF target) and BID in both lines tested, but BAX was only upregulated in OPM-2.

Since we observed differential oxygen-dependent expression patterns for the HIF α -subunits, we next asked if expression in the PHD isoforms responsible for regulating the α -subunits could explain these results. As seen in Fig 2A, expression of PHD2/EGLN1 was absent in 8226, but strongly expressed in OPM-2 cells. It has been reported that PHD2/EGLN1 preferentially hydroxylates HIF1 α (28), and its absence would explain why 8226 cells express constitutive HIF1 α under normoxic conditions. Along similar lines, we also found that PHD3/EGLN3, which preferentially hydroxylates HIF2 α (29), was absent in both 8226 and OPM-2 cells, and that also explains the oxygen-independent expression of HIF2 α in both these cell lines. To ensure that our antibodies could identify PHD/EGLN3 antigens, we included a positive internal EGLN3 control (EGLN3 overexpressing lysate from HEK293T cells purchased from NOVUS) in our immunoblots. We also found that low pO₂ (0.1%) significantly upregulated PHD2/EGLN1 protein expression, and probably this likely acts as a negative feedback mechanism to return HIF back to basal levels when O₂ levels return back to normal (30). Furthermore, hypoxia-mediated upregulation of PHD2/EGLN1 was unaffected by treatment with HIF-PA. We also examined the expression of another O₂-dependent regulator of HIF1 α , the factor inhibiting HIF-1 protein (FIH), and found that there was no difference in expression under either normoxic or hypoxic conditions in the cell lines we tested.

To further characterize the expression patterns of *PHD2/EGLN1*, we used the OncoPrint tool, a publically available cancer microarray database to query if there were differences in gene expression in clinical specimens of MM or monoclonal gammopathy of undetermined significance (MGUS) versus normal controls within two data sets; Zhan et al (N=78 samples) (31) and Agnelli et al (N=158) (32). As shown in Figure 2B, *PHD2/EGLN1* (top panel) was significantly overexpressed in MM specimens versus normal specimens (p<0.05), and in MGUS versus normal specimens in the Zhan study (p<0.05) but not in the Agnelli study (p>0.05). On the other hand, *PHD3/EGLN3* (bottom panel) was not

significantly different in MM and MGUS versus normal specimens ($p > 0.05$) in either data set, although there was a general downward trend of expression of this gene. Next, we used the TaqMan® Array Human Hypoxia 96-well assay system to analyze for changes in a subset of hypoxia-related genes in 8226 cells. As shown in Fig 2C, hypoxia increased the relative expression of *HIF1 α* by 6 fold, but had only minor effects on *HIF2 α* expression, mirroring the results shown in Fig 1B. Other genes associated with the HIF regulatory pathway, such as *PHD2/EGLN1*, *cullen-2* and *EP300*, were induced, whilst *PHD3/EGLN3* and *E3 ubiquitin* were downregulated and which mirrored the results from Fig 2A and 2B above. Not unexpectedly, *VEGF* and *angiopoietin-4* gene expression, genes that are well known to be sensitive to hypoxia, were upregulated by hypoxia.

HIF-targeting polyamide (HIF-PA) inhibits the adaptive hypoxic response in MM cells

We next tested the ability of HIF-PA to inhibit the cellular response to hypoxia using 8226 cells that had been stably transduced with a hypoxia response element (HRE)-luciferase reporter construct (8226-HRE-LUC). As shown in Fig 3A, culturing 8226-HRE-LUC cells under low pO_2 (0.1% O_2 , 24hr) resulted in a ~2 fold induction of luciferase activity over the baseline “normoxic” controls. This hypoxia-mediated LUC induction was significantly inhibited ($p < 0.05$) by treatment with HIF-PA but not by a control polyamide (CO-PA) that recognized a non-HRE sequence. To provide further support for our model, we knocked down HIF1 α expression in 8226-LUC cells using HIF1 α siRNA (Fig 3B top panel). As we expected, and as shown in Fig 3B (bottom panel), the hypoxia-mediated increase of LUC activity in 8226-LUC reporter cells transfected with HIF1 α siRNA also demonstrated a significant inhibition of the hypoxia-induced LUC activity. These data support our hypothesis that HIF-PA can specifically inhibit the HIF-mediated cellular response to hypoxia in 8226 cells. Next we showed that HIF-PA could inhibit the expression of HIF-mediated gene expression using real-time PCR to assay for the effect of HIF-PA treatment on the expression VEGF RNA. It is well known that hypoxia upregulates VEGF transcription in myeloma cells, and as expected, culturing 8226 cells under hypoxic conditions (0.1% O_2 , 24 hrs) induced VEGF mRNA by ~3–4 fold (Fig 3C). Treatment with HIF-PA significantly ($p < 0.05$) inhibited this hypoxia-mediated upregulation of VEGM mRNA in a dose dependent manner. This effect on mRNA was also mirrored by HIF-PA mediated inhibition of VEGF protein (measured by ELISA) in the supernatant of these cells (Fig 3D). Altogether, these data demonstrate that HIF-PA specifically and effectively inhibits the adaptive hypoxic response in MM cells.

HIF-PA treatment overcomes MM cell resistance to hypoxia

We next asked if inhibiting the hypoxic response with HIF-PA could sensitize a panel of MM cells to hypoxia-mediated killing. We assayed this using hypoxia resistant 8226 and U266 cells and hypoxia sensitive MM1.S and OPM-2 cells that were cultured under normoxic or hypoxic conditions (0.1% O_2) in the presence of HIF-PA or a control polyamide (CO-PA). HIF-PA had little effect on 8226 cells (Fig 4A) and U266 (Fig 4B) cultured under standard conditions (white bars), but the treatment of 8226 and U266 cells cultured under hypoxic conditions resulted in significant and dose-dependent hypoxia-mediated killing (an increase from ~20% to ~60%) (black bars) (ANOVA * $p < 0.05$). The hypoxia “sensitive” MM1.S and OPM-2 cells (Fig 4C and D) were even more responsive to

HIF-PA, (ANOVA * $p < 0.05$) with a similar increase in apoptosis observed by only 24 hrs when cultured under low O_2 conditions. The CO-PA compound had little, if any, effect on the hypoxia-mediated apoptosis in any of the cell lines examined. These data support our hypothesis that inhibiting the adaptive hypoxic response with HIF-PA overcomes MM resistance to hypoxia-mediated apoptosis *in vitro*.

As an *in vivo* correlate of the above *in vitro* data, we tested HIF-PA activity using a xenograft SQ MM tumor model in NOD/SCID mice (21, 24, 33). The mice were challenged on the flank with 10×10^6 8226 cells admixed with matrigel. Once a palpable tumor developed (~15 days later), the mice were randomized into groups (N=10 mice/group) to be given 5 IP injections of either HIF-PA (100 nmol/injection) or vehicle control every other day (Fig 5A, arrows on X-axis indicate days of treatment). The HIF-PA treatments were well tolerated, with only a small transient decrease in weight being observed, and induced a rapid and significant inhibition of tumor growth in the HIF-PA-treated mice compared to control mice ($p < 0.05$). In order to confirm uptake of HIF-PA, we treated an additional group of mice (N=2 mice/group) with a FITC-conjugated HIF-PA and measured drug uptake by real-time fluorescent imaging. We observed some auto-fluorescence signal in the bladder and gut (Supplemental Figure 1A, mice #1 and #2). However, in FITC-HIF-PA treated mice, positive signals were also observed in the tumor nodules (Supplemental Figure 1A, note arrow indicating tumor nodule in mouse #3 and #4). Labeled HIF-PA localization in the nuclei was confirmed by fluorescent confocal microscopy of excised tumor sections, costained with DAPI (Supplemental Figure 1B). This is consistent with the recent studies on the uptake C^{14} labeled Py-Im polyamides into tumors (34)

In order to characterize the *in vivo* effect of HIF-PA, we excised the tumor nodules 24 hrs after the last injection and performed immunohistochemistry on serial sections stained either for hypoxia (pimonidazole staining, left panels) or apoptosis (cleaved caspase 3, right panels) (Fig 5B). Both vehicle control (top left panel) and HIF-PA (bottom left panel) treated tumors had regions of hypoxia (brown stained areas), but the extent of hypoxia was significantly greater in the HIF-PA treated tumors than in the control tumors (quantified in Fig 5C). We also noted there were significantly greater areas of necrosis within the tumor bed in HIF-PA treated tumors compared to control tumors as well as a strong physical correlation between areas of hypoxia and presence of apoptosis in the HIF-PA-treated tumors (see Fig 5B, bottom right panel). In contrast, apoptotic cells were evenly distributed throughout the tumor bed in the control tumors (Fig 5B, top right panel) and were not localized to a specific geographic region in the tumor. As shown in Fig 5C, we found that the area of positive hypoxia staining in tumor sections (10 tumors/group, 10 fields/tumor) was ~35% in nodules harvested from the HIF-PA treated mice, compared to about 18% in the tumors harvested from mice treated with vehicle control ($p < 0.05$). The apoptotic index (AI) in both the normoxic or hypoxic regions of the tumor was determined by counting number of apoptotic cells in these regions using corresponding serial sections (10 tumors/group, 10 fields/region) stained with pimonidazole to identify the specific geographical regions of interest. As shown in Fig 5D, there was an approximate 3–4 fold increase in apoptotic cells located within the hypoxic regions of tumors from the HIF-PA treated mice compared to hypoxic regions of the control tumors ($P < 0.05$), whilst there was no difference

in apoptotic index within “normoxic” regions of the tumor bed. Finally, we examined the expression of VEGF in tumor lysates by ELISA (Fig 5E). As with our *in vitro* data (see Fig 3D), HIF-PA significantly inhibited VEGF expression by approximately 50% when compared to control tumors. Altogether, this data supports our hypothesis that HIF-PA can overcome resistance to hypoxia-mediated apoptosis *in vivo* by inhibiting the adaptive hypoxic response.

As a more physiologically relevant model, we developed an orthotopic, “disseminated” bone marrow-engrafted xenograft model based on the model developed by Miyakawa (35) using LUC2-transfected 8226 (these cells use a different p4.5 LUC2 plasmid to drive luciferase expression and thus are different than the 8226-HRE-LUC cells described above) allowing us to perform real-time longitudinal studies on myeloma tumors engrafted in the BM. As shown in Supplemental Fig 1A, NOG mice challenged with 8226LUC cells developed bone marrow engrafted MM tumors that could be observed by bioluminescence (top panel) and X-ray (bottom panel) analysis. Approximately 20–50% of the bone marrow cells from inoculated mice were positive for human CD45 confirmed by flow cytometry using FITC-conjugated anti-huCD45 antibody (Supplemental Fig 2B) and by IHC of *in situ* huCD45+ 8226 cells in the mouse femurs (Supplemental Fig 2C). Gross histological analysis of the mice didn’t show tumor formation in other tissues (i.e. liver, lung, spleen, or kidney).

We then asked if treatment with HIF-PA had an anti-MM effect on tumor cells in the bone marrow. As shown in Fig 6A, approximately +20 days post challenge with 8226-LUC cell, engraftment of LUC2+ cells in the skeleton was confirmed and the mice were then randomized into treatment groups (6–8 mice/group). The mice were then give IP injections of 100 nmol/injection of HIF-PA every other day (arrows indicate days of injection on day +27, +29 +31, +34, +36 and +38) or vehicle control. The average radiance (photons/sec/cm²/steradian) was measured at various time points using a Perkin Elmer Lumina XRMS small animal imager (out to day +40). The treatment with HIF-PA significantly inhibited MM tumor growth in the marrow (data is presented as average radiance \pm 95% confidence intervals) starting after the third injection and reaching statistical significance by the last HIF-PA injection on day +38). It should be noted that this particular HIF-PA treatment regimen was not able to delay the development of hind limb paralysis (the main end point criteria) when compared to control animals, with ~50% of the animals reaching their end point on day +59 (control mice) and day +62 (HIF-PA treated mice). Representative images of some of the mice are shown for day +22, +35 and +40. We noted a decrease in the luciferase activity as well as a general shrinkage of individual tumor foci in the mice. Specifically, in control mice, tumor foci tended to grow and merge over time, while in HIF-PA treated mice, the foci remain relatively small and isolated.

Effect of targeting the mTOR pathway on regulation of HIF-PA sensitivity

Since we have previously demonstrated that mammalian target of rapamycin (mTOR) inhibitors kill MM cells *in vivo*, and this anti-MM effects is mediated, at least in part, by inhibiting VEGF translation and *de novo* angiogenesis (21, 24, 33, 36), we asked if there would be a synergistic effect if we combined HIF-PA-mediated inhibition of hypoxia-inducible gene transcription in combination with rapamycin-mediated inhibition of mTOR-

mediated regulation of protein translation. As shown in Fig 7A, treatment of 8226 cells with the mTOR inhibitor rapamycin had a modest effect on apoptosis in MM cells cultured under normoxic or hypoxic conditions (0.1% O₂, 72 hours). However, under low pO₂ conditions, using median effect combination indices (CI) analysis for apoptosis induction, we found that the combination treatment with rapamycin and HIF-PA resulted in synergistic drug interactions with CI values <1 across several concentrations tested. Altogether, this suggests that targeting both transcription and translation of hypoxia-induced genes may be an effective anti-MM strategy (Fig 7A see grey and black bars and bracketed area). We also asked if REDD1, a hypoxia-sensitive negative regulator of mTOR, was affected by low pO₂ in both 8226 and OPM-2 cells. As shown in Fig 7B, REDD1 was strongly induced in MM cells. Furthermore, the functional effects of hypoxia on mTOR signaling demonstrated a marked inhibition of phosphorylation of p70S6 kinase but only modest effects on AKT phosphorylation. The effects of hypoxia-mediated inhibition on p70 was transient and reversible in OPM-2 cells, with p70 (389) phosphorylation levels rapidly returning to normal within 2 hrs following reoxygenation of the cells (Fig 7C).

Discussion

There is increasing evidence that low oxygen conditions are supportive of MM growth, progression and the development of resistance to chemotherapy, and that this occurs via a cellular adaptive hypoxic response mediated, at least in part, by the action of HIF-transcriptional factors. Because of this and the development of more resistant tumor phenotypes associated with hypoxia, there has been increasing interest in targeting HIF-mediated gene transcription to overcome these effects (18). Hypoxia induces the expression of about ~100–200 genes mostly related to metabolism, angiogenesis, and apoptosis (37, 38), and in this study, we found that a sequence-specific DNA-binding oligomer (HIF-PA) that is capable of binding to the HRE and inhibiting HIF-mediated gene transcription (19, 39) can overcome MM resistance to hypoxia-mediated apoptosis *in vitro* and *in vivo*. We also found that treating MM cells with a combination of HIF-PA, to inhibit gene transcription, and rapamycin, to inhibit gene translation, had a strong synergistic cytotoxic effect against MM tumor cells cultured under hypoxic conditions. Our results provide a strong pre-clinical rationale for using polyamides to target the adaptive hypoxic response in MM and may prove to be efficacious in treating myeloma tumors engrafted in the hypoxic bone marrow microenvironment. We also note that the ability of HIF-PA to recognize and bind to HRE sequences enables them to block both the HIF1 α /HIF1 β and HIF2 α /HIF1 β dimers.

We surveyed a panel of MM cell lines and found that the expression of the HIF1 α -subunit was generally absent under normal culturing conditions but was rapidly increased by low pO₂ levels. The exception to this was 8226 cells, which constitutively expressed HIF1 α under normoxic conditions, although it was further upregulated by hypoxia. In contrast to the HIF1 α -subunit, HIF2 α was constitutively expressed in all the cell lines studied (except MM1S), and the expression levels were independent of O₂ levels. Of note, we did not observe a correlation between the expression of the HIF1 α -subunit and sensitivity to hypoxia-mediated cytotoxicity in the cells we examined. These results are interesting because they suggest that the HIF α -subunits are differentially regulated by low pO₂ levels in

MM cells and that mechanisms other than just the expression of HIF1 α regulates sensitivity to hypoxia. In fact, despite their similarities, it is known that the α -subunits can mediate different responses to hypoxia and tumorigenesis: HIF1 α acts as a tumor suppressor gene and inhibits tumor growth, whilst HIF2 α acts as an oncogene and promotes tumor growth (3, 40). It has also been demonstrated that the different α -subunits have varying affinities for hydroxylation by the different PHD isoforms, with PHD2/EGLN1 showing the highest affinity for HIF1 α (28) and PHD3/EGLN3 showing the highest affinity for HIF-2 α (29). In our study, we found that the expression patterns of PHD/EGLN isoforms could explain HIF α -subunit expression in both 8226 and OPM-2 cells. Specifically, PHD2/EGLN1 was expressed at very low levels in 8226, but not in OPM-2, which can explain why HIF1 α was constitutively expressed in the former but not the later. It is also likely that the absence of PHD3/EGLN3 in MM cells results in the inability to hydroxylate HIF2 α , thereby rendering its expression independent of O₂ levels. Thus, it is likely that the expression and ability of PHD isoforms to regulate the expression of the different α -subunits may have important ramifications for disease progression and pathology in MM, such as what is observed in patients with VHL-cancer syndrome (41). In support of this, *PHD3/EGLN3*, but not *PHD2/EGLN1* silencing has been reported at a relatively high frequency for patients with MM, Waldenström's macroglobulinaemia and monoclonal gammopathy of undetermined significance and that these patients have a poorer prognosis (42) suggesting that PHD/EGLN activity is as important as HIF activity in regulating the adaptive hypoxic responses in MM, and is something that we will pursue in future experiments.

There is a dynamic physiological process that exists between the metabolic needs of tumor cell growth and the sufficiency of the vascular networks that are required to support these needs. On one hand, the development of oxygen stress within the tumor inhibits cell division and growth and induces cell death, but on the other hand, hypoxia activates the HIF-mediated cellular responses that provide protective growth and survival advantages and that can foster the development of tumor resistance to radiation and chemotherapy (27, 43). In this study, we found that HIF-PA was well tolerated by mice, localized to the nuclei of the tumor xenografts, and could inhibit tumor growth. Histological analysis of HIF-PA treated SQ xenografts indicated that tumor cytotoxicity was remarkably co-localized with regions of ischemic stress in the tumor nodules and that VEGF expression was significantly inhibited. While VEGF is clearly a factor in the induction of the HIF-PA-mediated killing of MM tumor cells, we believe that VEGF is probably only one of many genes affected by targeting the adaptive hypoxic response using HIF-PA (39). While our SQ model demonstrated some efficacy of HIF-PA in reducing solid MM xenograft tumors, we recognize that this particular model may not be physiologically relevant to clinical myeloma, which engrafts in the bone marrow. Therefore, we also present data using an orthotopic MM xenograft model. In this model, 8226 tumor cells localized to the mouse BM demonstrate a similar anti-tumor response to HIF-PA treatment that mirrored the effects seen in our SQ model. Specifically, we noted a decrease in luciferase activity measured by the change in average radiance, as well as a general decrease in the size of the MM tumor foci engrafted in the bone marrow. While HIF-PA had a statistically significant effect on orthotopic MM tumors, this did not translate to a longer survival in the mice. We believe that this may be because our initial HIF-PA treatment strategy was not the most effective dosing regimen for establishing and

maintaining long term anti-myeloma responses in our orthotopic model. For example, HIF-PA availability and clearance in the bone marrow still needs to be established. This, in fact, has important ramifications for addressing the known limitations of these anti-angiogenesis therapies (44), because HIF-PA directly targets the hypoxic response at the level of gene transcription, rather than targeting a single downstream effector of hypoxia, such as VEGF.

Because of our previous *in vivo* studies (21, 24, 33, 36) that demonstrated a correlation between the anti-angiogenic effects of the mTOR inhibitor, temsirolimus, we initially hypothesized that hypoxic stress alone would be sufficient to kill MM cells. However, we found that MM cell lines are generally resistant to low O₂, suggesting that hypoxia-induced physiological stress alone cannot fully explain our results. In fact, myeloma cells that are the most resistant to mTOR inhibition (e.g. 8226 and U266), are also the most resistant to hypoxia, whilst cells that are more sensitive to rapalogs, such as OPM-2 are the most sensitive hypoxia-mediated killing (45). It is also known that hypoxia regulates the activity of mTOR via the induction of REDD1 (46) although the relationship between hypoxia, mTOR activation, and HIF expression/activation remain complex and is not fully understood (47). This is further confounded by the presence of cap-independent, IRES-mediated translational pathways (48, 49) that may allow tumor cells to escape mTOR-targeting therapies. Interestingly, we find that the combination of polyamides and rapamycin can effectively synergize with each other to overcome resistance to hypoxia-mediated killing of 8226 cells *in vitro*. Along another line of reasoning, we noted that in a recent study by Maiso et al (10), hypoxic conditions conferred a striking resistance to bortezomib-mediated apoptosis in MM cell lines and, critically, inhibiting HIF1 α expression could restore sensitivity. If true, then we hypothesized that HIF-PA would likely have a similar effect in bortezomib-treated cells by inhibiting the adaptive hypoxic response and overcoming any hypoxia-mediated resistance to this drug. However, despite our best efforts, we were unable to replicate this phenomenon, and instead found that our results were more similar to those reported by Hu et al (50) which found instead that bortezomib killed MM cell lines cultured under hypoxic conditions. It is unclear why our experiments differed from those of Maiso et al, but could reflect variations in how hypoxic conditions were established. Therefore, at least in our hands, it remains to be shown if hypoxia confers resistance to chemotherapeutic drugs and if HIF-PA can overcome and sensitize MM cells by inhibiting HIF-activity.

In summary, HIF and related hypoxic response factors are frequently upregulated in MM tumors, and has been implicated in contributing to the development and prognosis of MM (15). The induction of pro-angiogenic, proliferative, metastatic, and glycolytic genes by HIF1 may also be involved in the development of chemotherapy resistant phenotypes (10, 27). In this sense, HIF1, and in particular the expression of the different α -subunits, may play dual roles in the survival and progression of MM, through the differential α -subunit expression patterns and the genes that they activate. Thus, we argue that understanding the role and mechanisms HIF1-mediated adaptive hypoxic response at the level of HIF1/DNA binding could be clinically relevant for developing novel therapies against patient MM engrafted in the hypoxic bone marrow environment.

Supplementary Material

Refer to Web version on PubMed Central for supplementary material.

Acknowledgments

GRANT SUPPORT

This work was supported by a MERIT grant 1I01BX001532 to PJF, from the United States Department of Veterans Affairs Biomedical Laboratory Research and Development Service and a NIH GM051747 grant to PBD

Literature Cited

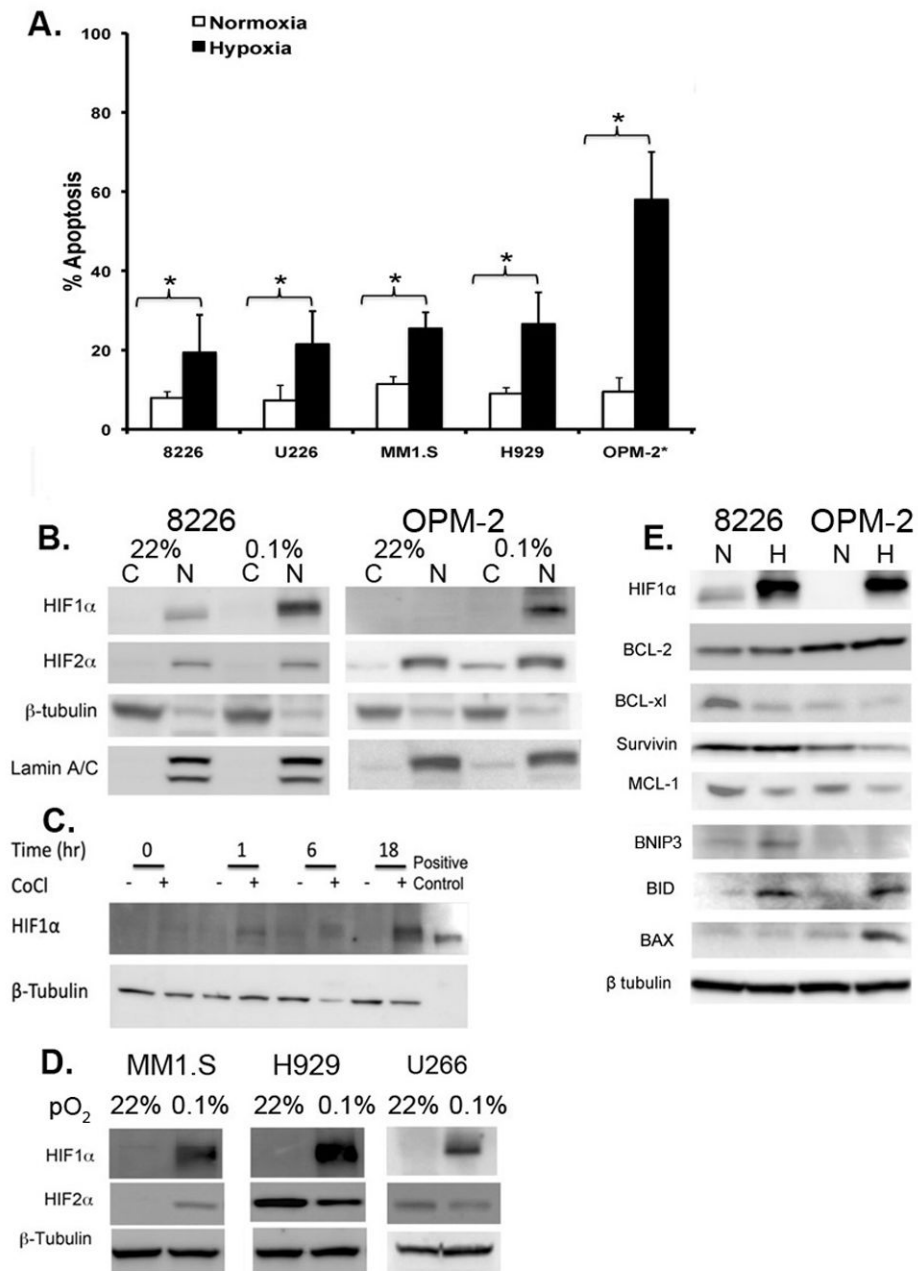
1. Kumar SK, Rajkumar SV, Dispenzieri A, Lacy MQ, Hayman SR, Buadi FK, Zeldenrust SR, Dingli D, et al. Improved survival in multiple myeloma and the impact of novel therapies. *Blood*. 2008; 111(5):2516–20. [PubMed: 17975015]
2. Lonial S, Mitsiades CS, Richardson PG. Treatment options for relapsed and refractory multiple myeloma. *Clin Cancer Res*. 2011; 17(6):1264–77. [PubMed: 21411442]
3. Martin SK, Diamond P, Gronthos S, Peet DJ, Zannettino AC. The emerging role of hypoxia, HIF-1 and HIF-2 in multiple myeloma. *Leukemia*. 2011; 25(10):1533–42. [PubMed: 21637285]
4. Hideshima T, Chauhan D, Podar K, Schlossman RL, Richardson P, Anderson KC. Novel therapies targeting the myeloma cell and its bone marrow microenvironment. *Semin Oncol*. 2001; 28(6):607–12. [PubMed: 11740818]
5. Podar K, Chauhan D, Anderson KC. Bone marrow microenvironment and the identification of new targets for myeloma therapy. *Leukemia*. 2009; 23(1):10–24. [PubMed: 18843284]
6. Spencer JA, Ferraro F, Roussakis E, Klein A, Wu J, Runnels JM, Zaher W, Mortensen LJ, et al. Direct measurement of local oxygen concentration in the bone marrow of live animals. *Nature*. 2014; 508(7495):269–73. [PubMed: 24590072]
7. Hockel M, Vaupel P. Biological consequences of tumor hypoxia. *Semin Oncol*. 2001; 28(2 Suppl 8):36–41. [PubMed: 11395851]
8. Asosingh K, De Raeve H, de Ridder M, Storme GA, Willems A, Van Riet I, Van Camp B, Vanderkerken K. Role of the hypoxic bone marrow microenvironment in 5T2MM murine myeloma tumor progression. *Haematologica*. 2005; 90(6):810–7. [PubMed: 15951294]
9. Giatromanolaki A, Bai M, Margaritis D, Bourantas KL, Koukourakis MI, Sivridis E, Gatter KC. Hypoxia and activated VEGF/receptor pathway in multiple myeloma. *Anticancer Res*. 2010; 30(7): 2831–6. [PubMed: 20683019]
10. Maiso P, Huynh D, Moschetta M, Sacco A, Aljawai Y, Mishima Y, Asara JM, Roccaro AM, et al. Metabolic signature identifies novel targets for drug resistance in multiple myeloma. *Cancer Res*. 2015; 75(10):2071–82. [PubMed: 25769724]
11. Greer SN, Metcalf JL, Wang Y, Ohh M. The updated biology of hypoxia-inducible factor. *Embo J*. 2012; 31(11):2448–60. [PubMed: 22562152]
12. Fandrey J, Gorr TA, Gassmann M. Regulating cellular oxygen sensing by hydroxylation. *Cardiovascular research*. 2006; 71(4):642–51. [PubMed: 16780822]
13. Vacca A, Ribatti D, Roncali L, Ranieri G, Serio G, Silvestris F, Dammacco F. Bone marrow angiogenesis and progression in multiple myeloma. *Br J Haematol*. 1994; 87(3):503–8. [PubMed: 7527645]
14. Vacca A, Di Loreto M, Ribatti D, Di Stefano R, Gadaleta-Caldarola G, Iodice G, Caloro D, Dammacco F. Bone marrow of patients with active multiple myeloma: angiogenesis and plasma cell adhesion molecules LFA-1, VLA-4, LAM-1, and CD44. *Am J Hematol*. 1995; 50(1):9–14. [PubMed: 7545353]
15. Rajkumar SV, Leong T, Roche PC, Fonseca R, Dispenzieri A, Lacy MQ, Lust JA, Witzig TE, et al. Prognostic value of bone marrow angiogenesis in multiple myeloma. *Clin Cancer Res*. 2000; 6(8): 3111–6. [PubMed: 10955791]

16. Kumar S, Witzig TE, Dispenzieri A, Lacy MQ, Wellik LE, Fonseca R, Lust JA, Gertz MA, et al. Effect of thalidomide therapy on bone marrow angiogenesis in multiple myeloma. *Leukemia*. 2004; 18(3):624–7. [PubMed: 14749707]
17. White D, Kassim A, Bhaskar B, Yi J, Wamstad K, Paton VE. Results from AMBER, a randomized phase 2 study of bevacizumab and bortezomib versus bortezomib in relapsed or refractory multiple myeloma. *Cancer*. 2013; 119(2):339–47. [PubMed: 22811009]
18. Podar K, Anderson KC. A therapeutic role for targeting c-Myc/Hif-1-dependent signaling pathways. *Cell Cycle*. 2010; 9(9):1722–8. [PubMed: 20404562]
19. Olenyuk BZ, Zhang GJ, Klco JM, Nickols NG, Kaelin WG Jr, Dervan PB. Inhibition of vascular endothelial growth factor with a sequence-specific hypoxia response element antagonist. *Proc Natl Acad Sci U S A*. 2004; 101(48):16768–73. [PubMed: 15556999]
20. Belitsky JM, Nguyen DH, Wurtz NR, Dervan PB. Solid-phase synthesis of DNA binding polyamides on oxime resin. *Bioorg Med Chem*. 2002; 10(8):2767–74. [PubMed: 12057666]
21. Frost P, Moatamed F, Hoang B, Shi Y, Gera J, Yan H, Gibbons J, Lichtenstein A. In vivo antitumor effects of the mTOR inhibitor CCI-779 against human multiple myeloma cells in a xenograft model. *Blood*. 2004; 104(13):4181–7. [PubMed: 15304393]
22. LeBlanc R, Catley LP, Hideshima T, Lentzsch S, Mitsiades CS, Mitsiades N, Neuberger D, Goloubeva O, et al. Proteasome inhibitor PS-341 inhibits human myeloma cell growth in vivo and prolongs survival in a murine model. *Cancer Res*. 2002; 62(17):4996–5000. [PubMed: 12208752]
23. Raskatov JA, Nickols NG, Hargrove AE, Marinov GK, Wold B, Dervan PB. Gene expression changes in a tumor xenograft by a pyrrole-imidazole polyamide. *Proc Natl Acad Sci U S A*. 2012; 109(40):16041–5. [PubMed: 22988074]
24. Frost P, Berlinger E, Mysore V, Hoang B, Shi Y, Gera J, Lichtenstein A. Mammalian target of rapamycin inhibitors induce tumor cell apoptosis in vivo primarily by inhibiting VEGF expression and angiogenesis. *J Oncol*. 2013; 2013:897025. [PubMed: 23533410]
25. Rhodes DR, Yu J, Shanker K, Deshpande N, Varambally R, Ghosh D, Barrette T, Pandey A, et al. ONCOMINE: a cancer microarray database and integrated data-mining platform. *Neoplasia*. 2004; 6(1):1–6. [PubMed: 15068665]
26. Martin SK, Diamond P, Williams SA, To LB, Peet DJ, Fujii N, Gronthos S, Harris AL, et al. Hypoxia-inducible factor-2 is a novel regulator of aberrant CXCL12 expression in multiple myeloma plasma cells. *Haematologica*. 2010; 95(5):776–84. [PubMed: 20015878]
27. Hu Y, Kiritto K, Yoshida K, Mitsumori T, Nakajima K, Nozaki Y, Hamanaka S, Nagashima T, et al. Inhibition of hypoxia-inducible factor-1 function enhances the sensitivity of multiple myeloma cells to melphalan. *Mol Cancer Ther*. 2009; 8(8):2329–38. [PubMed: 19671732]
28. Berra E, Benizri E, Ginouves A, Volmat V, Roux D, Pouyssegur J. HIF prolyl-hydroxylase 2 is the key oxygen sensor setting low steady-state levels of HIF-1alpha in normoxia. *EMBO J*. 2003; 22(16):4082–90. [PubMed: 12912907]
29. Bishop T, Gallagher D, Pascual A, Lygate CA, de Bono JP, Nicholls LG, Ortega-Saenz P, Oster H, et al. Abnormal sympathoadrenal development and systemic hypotension in PHD3^{-/-} mice. *Mol Cell Biol*. 2008; 28(10):3386–400. [PubMed: 18332118]
30. Fong GH, Takeda K. Role and regulation of prolyl hydroxylase domain proteins. *Cell Death Differ*. 2008; 15(4):635–41. [PubMed: 18259202]
31. Zhan F, Barlogie B, Arzoumanian V, Huang Y, Williams DR, Hollmig K, Pineda-Roman M, Tricot G, et al. Gene-expression signature of benign monoclonal gammopathy evident in multiple myeloma is linked to good prognosis. *Blood*. 2007; 109(4):1692–700. [PubMed: 17023574]
32. Agnelli L, Mosca L, Fabris S, Lionetti M, Andronache A, Kwee I, Todoerti K, Verdelli D, et al. A SNP microarray and FISH-based procedure to detect allelic imbalances in multiple myeloma: an integrated genomics approach reveals a wide gene dosage effect. *Genes Chromosomes Cancer*. 2009; 48(7):603–14. [PubMed: 19396863]
33. Frost P, Shi Y, Hoang B, Lichtenstein A. AKT activity regulates the ability of mTOR inhibitors to prevent angiogenesis and VEGF expression in multiple myeloma cells. *Oncogene*. 2007; 26:2255–62. [PubMed: 17016437]

34. Raskatov JA, Puckett JW, Dervan PB. A C-14 labeled Py-Im polyamide localizes to a subcutaneous prostate cancer tumor. *Bioorg Med Chem*. 2014; 22(16):4371–5. [PubMed: 24780272]
35. Miyakawa Y, Ohnishi Y, Tomisawa M, Monnai M, Kohmura K, Ueyama Y, Ito M, Ikeda Y, et al. Establishment of a new model of human multiple myeloma using NOD/SCID/gammac(null) (NOG) mice. *Biochem Biophys Res Commun*. 2004; 313(2):258–62. [PubMed: 14684154]
36. Frost P, Shi Y, Hoang B, Gera J, Lichtenstein A. Regulation of D-cyclin translation inhibition in myeloma cells treated with mammalian target of rapamycin inhibitors: rationale for combined treatment with extracellular signal-regulated kinase inhibitors and rapamycin. *Mol Cancer Ther*. 2009; 8(1):83–93. [PubMed: 19139116]
37. Pouyssegur J, Dayan F, Mazure NM. Hypoxia signalling in cancer and approaches to enforce tumour regression. *Nature*. 2006; 441(7092):437–43. [PubMed: 16724055]
38. Semenza GL. Oxygen sensing, homeostasis, and disease. *N Engl J Med*. 2011; 365(6):537–47. [PubMed: 21830968]
39. Nickols NG, Jacobs CS, Farkas ME, Dervan PB. Modulating hypoxia-inducible transcription by disrupting the HIF-1-DNA interface. *Acs Chemical Biology*. 2007; 2(8):561–71. [PubMed: 17708671]
40. Raval RR, Lau KW, Tran MG, Sowter HM, Mandriota SJ, Li JL, Pugh CW, Maxwell PH, et al. Contrasting properties of hypoxia-inducible factor 1 (HIF-1) and HIF-2 in von Hippel-Lindau-associated renal cell carcinoma. *Mol Cell Biol*. 2005; 25(13):5675–86. [PubMed: 15964822]
41. Kaelin WG Jr. Molecular basis of the VHL hereditary cancer syndrome. *Nat Rev Cancer*. 2002; 2(9):673–82. [PubMed: 12209156]
42. Hatzimichael E, Dasoula A, Shah R, Syed N, Papoudou-Bai A, Coley HM, Dranitsaris G, Bourantas KL, et al. The prolyl-hydroxylase EGLN3 and not EGLN1 is inactivated by methylation in plasma cell neoplasia. *Eur J Haematol*. 2010; 84(1):47–51. [PubMed: 19737309]
43. Hu J, Handisides DR, Van Valckenborgh E, De Raeve H, Menu E, Vande Broek I, Liu Q, Sun JD, et al. Targeting the multiple myeloma hypoxic niche with TH-302, a hypoxia-activated prodrug. *Blood*. 2010; 116(9):1524–7. [PubMed: 20530289]
44. Sitohy B, Nagy JA, Dvorak HF. Anti-VEGF/VEGFR therapy for cancer: reassessing the target. *Cancer Res*. 2012; 72(8):1909–14. [PubMed: 22508695]
45. Shi Y, Gera J, Hu L, Hsu JH, Bookstein R, Li W, Lichtenstein A. Enhanced sensitivity of multiple myeloma cells containing PTEN mutations to CCI-779. *Cancer Res*. 2002; 62(17):5027–34. [PubMed: 12208757]
46. Brugarolas J, Lei K, Hurley RL, Manning BD, Reiling JH, Hafen E, Witters LA, Ellisen LW, et al. Regulation of mTOR function in response to hypoxia by REDD1 and the TSC1/TSC2 tumor suppressor complex. *Genes Dev*. 2004; 18(23):2893–904. [PubMed: 15545625]
47. Alam H, Weck J, Maizels E, Park Y, Lee EJ, Ashcroft M, Hunzicker-Dunn M. Role of the phosphatidylinositol-3-kinase and extracellular regulated kinase pathways in the induction of hypoxia-inducible factor (HIF)-1 activity and the HIF-1 target vascular endothelial growth factor in ovarian granulosa cells in response to follicle-stimulating hormone. *Endocrinology*. 2009; 150(2):915–28. [PubMed: 18845636]
48. Lang KJ, Kappel A, Goodall GJ. Hypoxia-inducible factor-1alpha mRNA contains an internal ribosome entry site that allows efficient translation during normoxia and hypoxia. *Mol Biol Cell*. 2002; 13(5):1792–801. [PubMed: 12006670]
49. Braunstein S, Karpisheva K, Pola C, Goldberg J, Hochman T, Yee H, Cangiarella J, Arju R, et al. A hypoxia-controlled cap-dependent to cap-independent translation switch in breast cancer. *Mol Cell*. 2007; 28(3):501–12. [PubMed: 17996713]
50. Hu J, Van Valckenborgh E, Xu D, Menu E, De Raeve H, De Bryune E, Xu S, Van Camp B, et al. Synergistic induction of apoptosis in multiple myeloma cells by bortezomib and hypoxia-activated prodrug TH-302, in vivo and in vitro. *Mol Cancer Ther*. 2013; 12(9):1763–73. [PubMed: 23832122]

Implications

Pyrrole-imidazole (Py-Im) polyamides target and disrupt the adaptive hypoxic responses in MM cells that may have clinical significance as a therapeutic strategy to treat myeloma engrafted in the bone marrow microenvironment.

**Figure 1.**

Cytotoxic effects of low pO₂ levels on myeloma cell lines. (A) The % apoptosis (measured by cleaved caspase 3) following 72 hour culture of myeloma cells under “normoxic” conditions (~22% O₂, 5% CO₂) or hypoxic (0.1% O₂, 5% CO₂) conditions, except for OPM-2 cells which were cultured for 48 hours. Brackets indicate P<0.05 (T-test). Values represent mean ± 1 standard deviation of 4 independent experiments/cell line. (B). Immunoblots of HIF1α and HIF2α-subunit expression in 8226 and OPM-2 cells cultured under normoxic or hypoxic conditions (0.1% O₂, 5% CO₂) for 24 hours. The cells were harvested on ice then the cytoplasmic and nuclear fractions were isolated, and the lysate was

immunoblotted for indicated proteins. C=cytoplasm fraction, N=nuclear fraction. The data presented are a representative immunoblots of at least 2 independent experiments. (C) Time course of CoCl₂-mediated induction of HIF1 α expression in OPM-2 cells. Cells were cultured with 100nM CoCl₂ or vehicle control and the cellular lysates were harvested at indicated time points and immunoblotted for HIF1 α expression. The data presented are a representative immunoblots of at least 2 independent experiments. (D) Hypoxia-mediated induction of HIF1 α and HIF2 α in MM1S, H929 and U266 myeloma cell lines cultured under normoxic or hypoxic (0.1% O₂, 5% CO₂) conditions for 24 hours. Cells were harvested on ice and the cell lysate was immunoblotted for HIF1 α and HIF2 α . The data presented are a representative immunoblots of at least 2 independent experiments. (E) Immunoblots showing hypoxia-mediated changes in survival-related protein expression in 8226 and OPM-2 cells cultured under normoxic or hypoxic conditions (0.1% O₂, 5% CO₂) for 24 hours. The cells were harvested on ice and the lysate was immunoblotted for indicated proteins. The data presented are a representative immunoblots of at least 2 independent experiments.

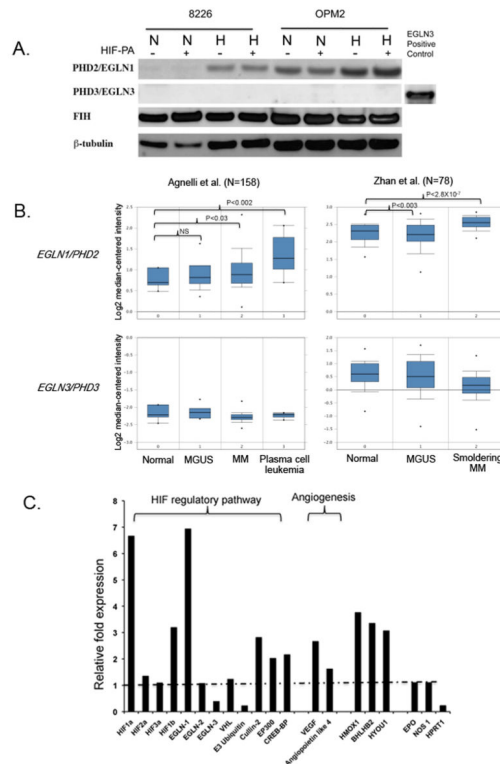


Figure 2.

There is differential expression of HIF regulatory pathway in 8226 cells. (A) Immunoblots of PHD2/EGLN1, PHD3/EGLN3 and FIH in 8226 cultured under normoxic or hypoxic conditions (0.1% O₂, 5% CO₂) for 48 hours in the presence or absence of HIF-PA (10 μ M). Cells were harvested on ice and the cell lysate was immunoblotted. A positive immunoblot control (an over expression lysate from HEK293T cells) for PHD3/EGLN3 is included. The data presented are a representative immunoblots of at least 2 independent experiments. (B) Boxplot results showing a meta-analysis of PHD2/EGLN1 and PHD3/EGLN3 in normal bone marrow, monoclonal gammopathy of undetermined significance (MGUS), multiple myeloma, smoldering myeloma and plasma cell leukemia. Analysis was performed using OncoPrint and includes two data sets: Agnelli et al (N=156) and Zhan et al (N=78). (C) Relative fold change in hypoxia-mediated expression of select genes compared to normoxic conditions. The 8226 cells were cultured under normoxic or hypoxic (0.1% O₂, 5% CO₂) conditions for 24 hours. The RNA was collected and gene expression was determined by quantitative real-time PCR analysis. The relative fold change in hypoxia-mediated gene expression compared to normoxic levels are shown. Values above the dotted line indicate upregulation of genes by hypoxia, and values below the dotted line indicate downregulation of genes by hypoxia. These data are representative of 2 independent experiments.

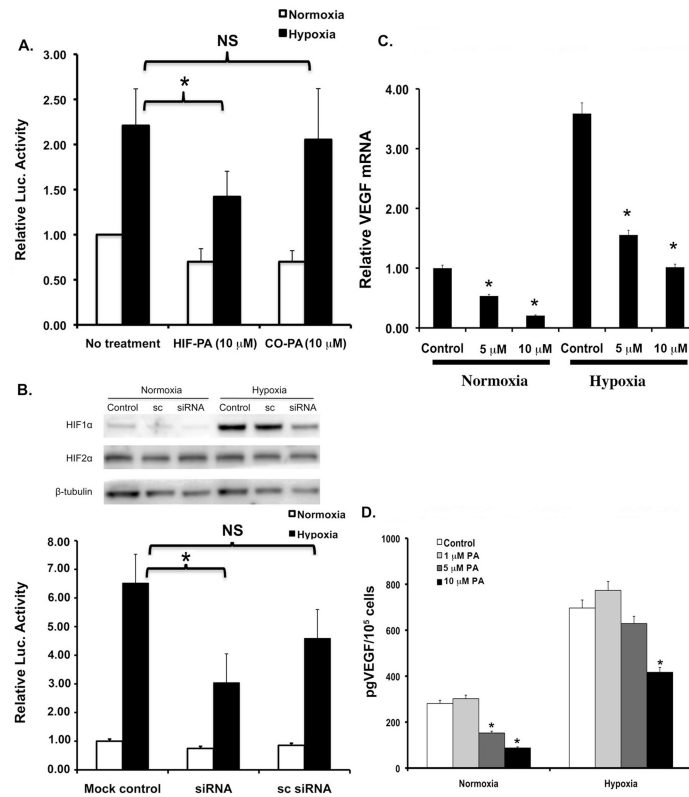
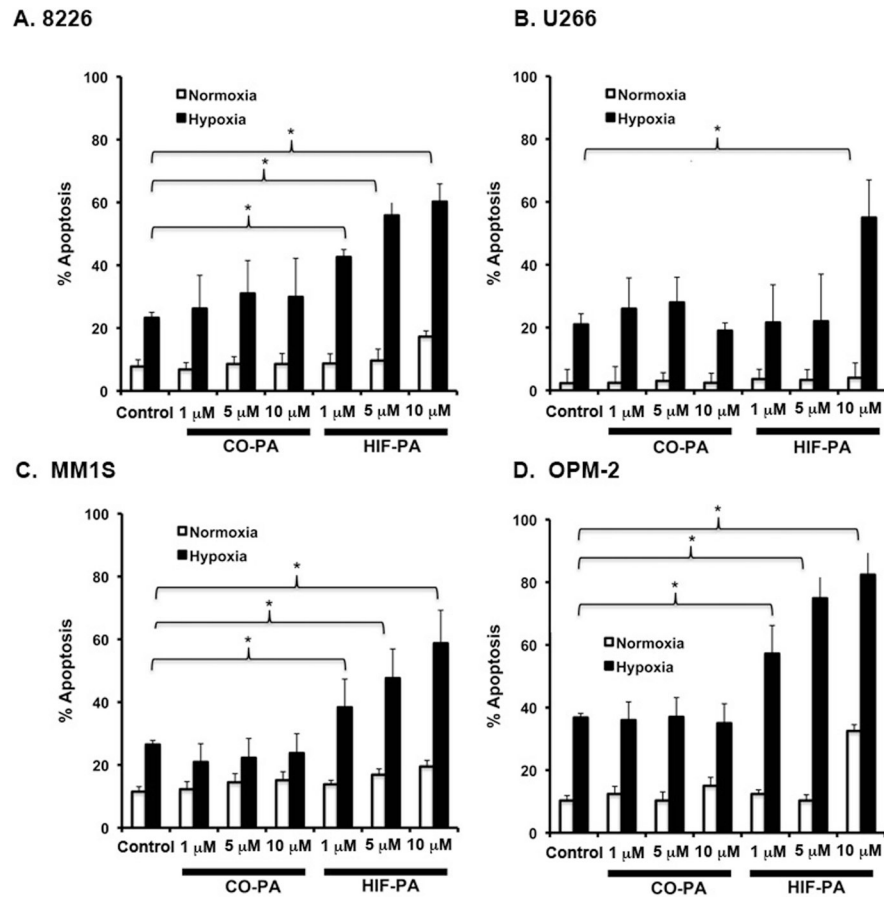
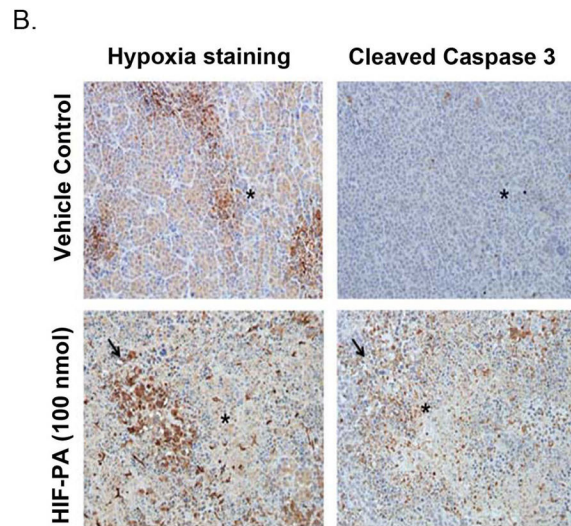
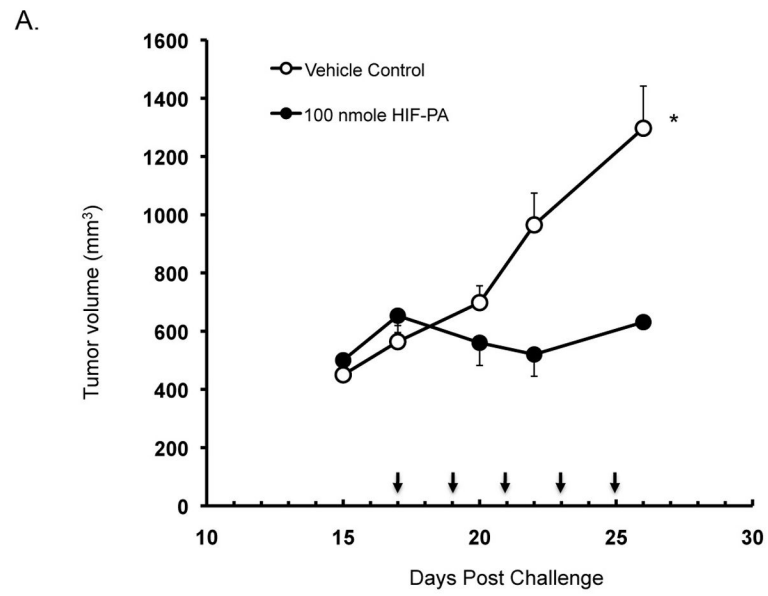


Figure 3. HIF-PA polyamide inhibits the *in vitro* response to low pO₂ in 8226 myeloma cell lines. (A) 8226-HRE-LUC reporter cells were cultured under normoxic or hypoxic (0.1% O₂, 5% CO₂) conditions and treated with either 10 μ M HIF-PA or 10 μ M CO-PA for 24 hours. Luciferase activity in cell extracts was measured using a luminometer. Values are presented as means \pm 1 standard deviation of 3 independent experiments. Bracket with *= P <0.05 (ANOVA). Bracket with NS= not significant. (B) 8226-HRE-LUC reporter cells were co-transfected with HIF1 α siRNA or scrambled (sc) control and were then cultured under normoxic or hypoxic (0.1% O₂, 5% CO₂) for 24 hours. Luciferase activity in cell extracts was measured using a luminometer. Values are presented as means \pm 1 standard deviation of 3 independent experiments. Bracket with *= P <0.05 (ANOVA). Bracket with NS= not significant. Top panel: Immunoblot demonstrating knockdown of HIF1 α (but not HIF2 α) by siRNA. These data are representative of 3 independent experiments. Bottom panel: Change in LUC activity in treated 8226 cells. Values are presented as means \pm 1 standard deviation of 3 independent experiments. Bracket with *= P <0.05 (ANOVA). Bracket with NS= not significant. (C) HIF-PA (10 μ M)-mediated inhibition of VEGF mRNA levels in 8226 cells cultured under normoxic or hypoxic (0.1% O₂, 5% CO₂) conditions for 24 hours. VEGF mRNA levels were measured by quantitative real-time PCR of 3 independent experiments. * P <0.05. (ANOVA). (D). Effect of HIF-PA treatment on VEGF protein in supernatants of 8226 cells cultured under normoxic or hypoxic conditions were measured by ELISA. Values are presented as mean \pm 1 standard deviation of 3 independent experiments. * P <0.05 (ANOVA).

**Figure 4.**

HIF-PA treatment sensitizes the hypoxia-resistant 8226, U266, and hypoxia-sensitive MM1S and OPM-2 cells to hypoxia-mediated apoptosis *in vitro*. (A) 8226 were cultured under normoxic or hypoxic (0.1% O₂, 5% CO₂) conditions with indicated concentration of HIF-PA or CO-PA for 72 hours. (B) U266 were cultured under normoxic or hypoxic (0.1% O₂, 5% CO₂) with indicated concentration of HIF-PA or CO-PA for 72 hours. (C) MM1S cells were cultured under normoxic or hypoxic (0.1% O₂, 5% CO₂) with indicated concentration of HIF-PA or CO-PA for 48 hours. (D) OPM-2 cells were cultured under normoxic or hypoxic (0.1% O₂, 5% CO₂) with indicated concentration of HIF-PA or CO-PA for 24 hours. At the end of the treatment, cells were harvested and the percent apoptosis was measured by flow cytometry for cleaved caspase 3. Values are mean \pm 1 standard deviation of 3 independent experiments. Bracket * indicates significant change (P<0.05) (ANOVA) of treatment compared to control.



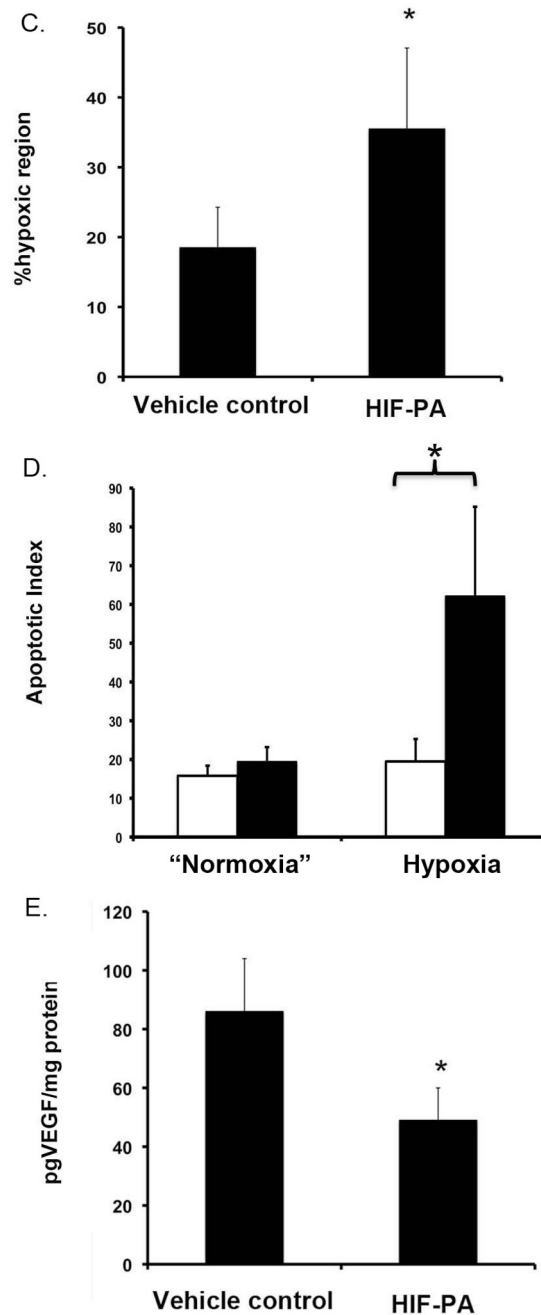


Figure 5. HIF-PA (100nmol/kg mouse) inhibits 8226 tumor growth in a subcutaneous (SQ) myeloma xenograft model (N=10 mice/group). (A) Change in 8226 tumor volume in HIF-PA-treated NOD/SCID mice. Mice were challenged SQ with 10×10^6 cells admixed in matrigel. When the tumor volume was $\sim 500 \text{ mm}^3$ (\sim day 15 post challenge), the mice were randomized into treatment and control groups (10 mice/group). The mice were given 5 IP injections at indicated concentration (Arrows indicate days of treatment) and the tumor volume was measured using calipers. Values represent mean volume \pm 95% confidence interval. *P<0.05. (B) Photomicrographs of SQ tumor sections harvested from mice treated with HIF-

PA or vehicle-control treated mice (N=10 mice/group). Tumors were harvested 24 hours after last the IP injections. Serial tumor sections were stained for hypoxia (by pimonidazole; brown stained areas) or apoptosis (cleaved caspase 3). *Indicate corresponding geographic regions in the sections. Arrow indicates areas of hypoxia and associated apoptosis. (C) The percent area of hypoxic tumor bed measured by staining with pimonidazole (measured in 10 fields/tumor, 10 tumors/group) in 8226 tumors harvested from HIF-PA or vehicle-treated mice. Area was measured using Metamorph computer software. Values are presented as mean \pm 1 standard deviation. *P<0.05. (ANOVA) (D) Apoptotic index (the number of apoptotic cells/unit area) was measured by counting cells staining for cleaved caspase 3 (10 fields/tumor, 10 tumors/group). The apoptotic index in regions of “normoxia” or “hypoxia” were assayed by using serial sections stained with pimonidazole to identify specific geographical areas in the tumor nodules. Values are presented as mean \pm 1 standard deviation. *P<0.05 (ANOVA). (E) Tumor lysate was collected and VEGF was analyzed by ELISA (10 tumors/group). Values are presented as mean \pm 1 standard deviation. *P<0.05 (T-test).

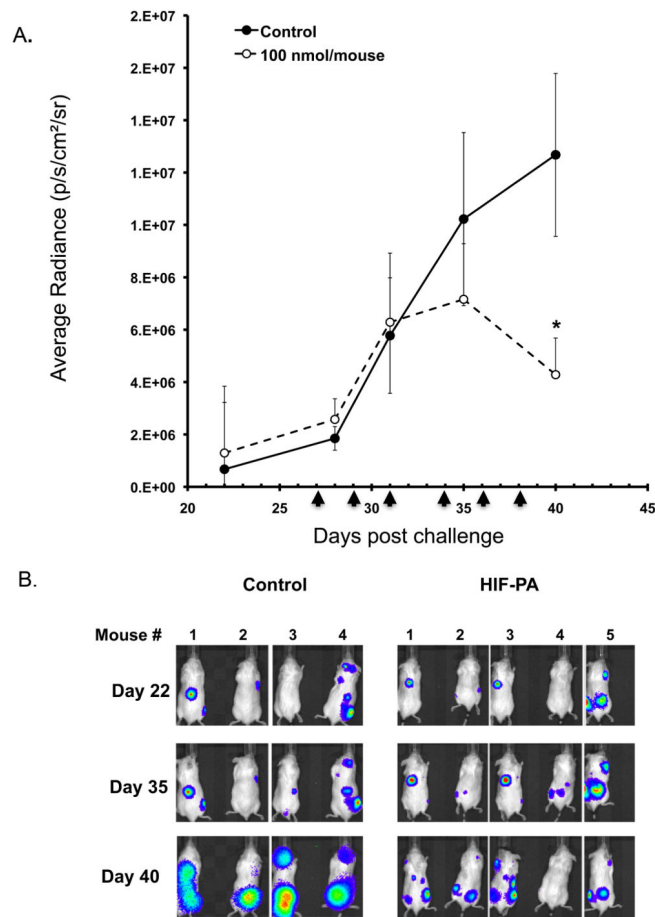
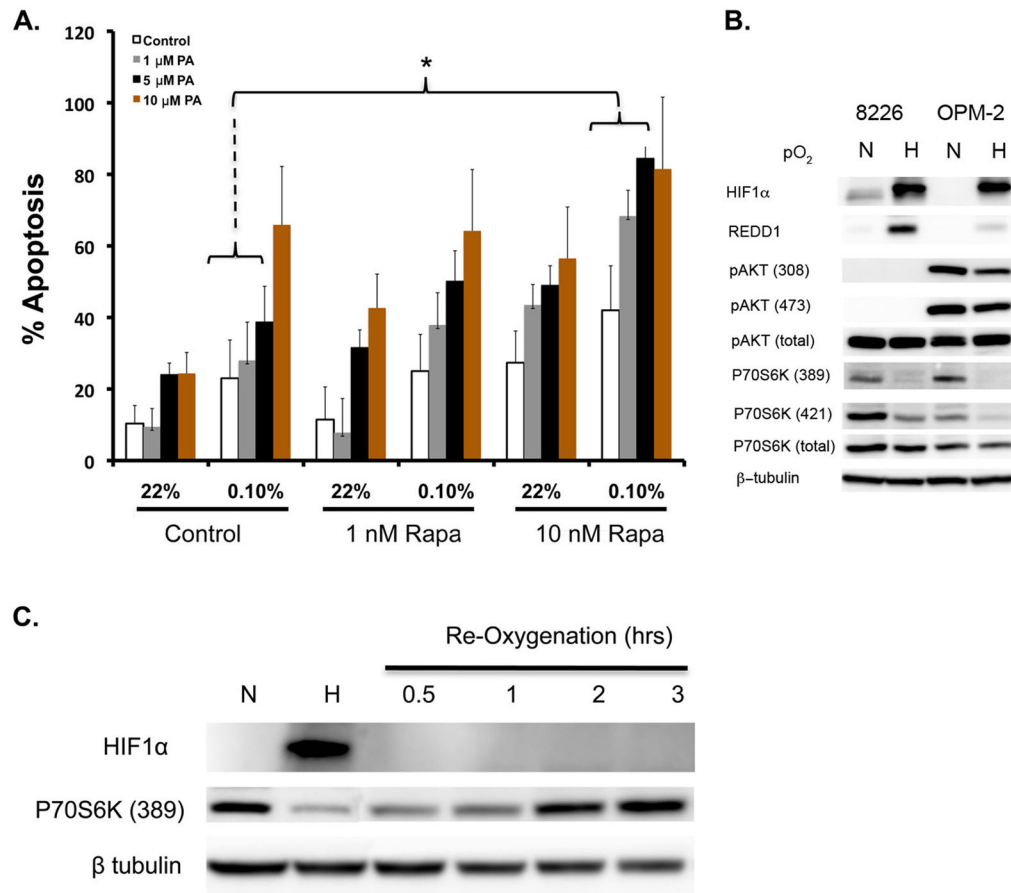


Figure 6.

HIF-PA (100nmol/kg mouse) inhibits 8226-LUC tumor growth in an orthotopic myeloma xenograft model (N=8 mice/group). (A) Change in average radiance (p/sec/cm²/ser) in HIF-PA-treated NOG mice was measured using IVIS XRMS small animal imaging system. Briefly, mice were challenged IV with 10×10^6 cells and engraftment of 8226-LUC cells were confirmed by IP injection of luciferin substrate (VivoGlo, Promega) starting ~day 20 post challenge. Once a positive signal was observed in the bone marrow, the mice were randomized into treatment and control groups (6–8 mice/group). The mice were given 6 IP injections at indicated concentration (Arrows indicate days of treatment) and the change in average radiance of tumor foci were measured as described above. Values represent mean volume \pm 95% confidence interval. *P<0.05. (B) Representative images of mice imaged on day +22, +35 and +40 showing changes in LUC activity. Mice were imaged using a IVIS XRMS small animal imaging system.

**Figure 7.**

Combination of rapamycin and HIF-PA can overcome resistance to hypoxia-mediated apoptosis in 8226 cells. (A) 8226 cells were cultured under normoxic (22% O₂, 5% CO₂) or hypoxic (0.1% O₂, 5% CO₂) and treated with the indicated concentrations of rapamycin, HIF-PA or both for 24 hours. At the end of the treatment, cells were harvested and % apoptosis was measured by flow cytometry for cleaved caspase 3. Values are mean \pm 1 standard deviation of 3 independent experiments. Bracket * indicates significant change (P < 0.05) of treatment compared to control (ANOVA). The effect of combining HIF-PA with rapamycin on induction of apoptosis was assessed by the median effect method using Calcsyn Software Version 1.1 (Biosoft, Cambridge, United Kingdom). Combination indices (CI) values were calculated using the most conservative assumption of mutually nonexclusive drug interactions. CI values were calculated from median results of apoptosis assays. (B) Immunoblots of mTOR-related signaling proteins in 8226 and OPM-2 cells cultured under normoxic or hypoxic conditions for 24 hours. The data presented are a representative immunoblots of at least 2 independent experiments. (C) Time course of p70S6 kinase phosphorylation in OPM-2 cells following re-oxygenation. Cells were cultured under hypoxic conditions (0.1% O₂, 5% CO₂) for 24 hours, then cultured under normoxic conditions (22% O₂, 5% CO₂). Cell lysates were harvested at indicated time points and

immunoblotted for HIF1 α and phospho-P79S6K (389) expression. The data presented are a representative immunoblots of at least 2 independent experiments.

Author Manuscript

Author Manuscript

Author Manuscript

Author Manuscript